HIERARCHICAL AND STATISTICAL ANALYSIS ON THE TENSILE STRENGTH OF SUPERCONDUCTING WIRE

Zhi-Yang Wang[1], Hua-Dong Yong[2] and You-he Zhou[3]

Key Laboratory of Mechanics on Environment and Disaster in Western China, The Ministry of Education of China, and Department of Mechanics and Engineering Sciences, College of Civil Engineering and Mechanics, Lanzhou University, Lanzhou, Gansu 730000, PR China
[1] wangzhy2015@lzu.edu.cn, [2] yonghd@lzu.edu.cn, [3] zhouyh@lzu.edu.cn

Keywords: Weibull distribution, statistical analysis, hierarchical, tensile strength, asymmetric structure

ABSTRACT

In this paper, we study the strength distribution of filament bundles in the superconducting wire. A hierarchical model is extended to analyze the stochastic strength of Bi2212 wire composite approximately. The Weibull function and shear-lag model are adopted to describe the filament strength and effective recovery length. The stress concentration factors are determined with the finite element analysis. Then the failure probability of higher level bundle which contains three lower level bundles is derived. After fitting the strength distribution of level-[i] bundle, the Weibull parameters can be updated and the failure probability of level-[i+1] can be obtained using the same approach. Finally, an asymmetric structure is considered. When one filament fails, the asymmetric structure will lead to the different stress concentration factors in the other two survival filaments, and the mean strength is also solved by modifying the model.

1 INTRODUCTION

Due to superconducting composite wires have high critical current density and high critical temperature [1], $Bi_2Sr_2Ca_1Cu_2O_{8+x}$ (Bi2212) superconducting composite wires have received much attention in recent years [2-7]. The critical current density can reach $400A/mm^2$ at high magnetic field 25 T [2, 3]. Bi2212 round wire is the candidate superconductor for the high filed magnet application which exceeds the limit of low temperature superconductor [4]. The superconducting Bi2212 round wire is a unidirectional fiber-reinforced composite. The composite contains Bi2212 filaments, matrix Ag and alloy sheath. There are many theoretical or experimental researches which considered the mechanical and electromagnetic characteristics in the Bi2212 wire [8-17]. It is well known that superconducting filament is brittle and isotropy [5]. The filament breakage will occur as the Lorentz force and mechanical loading are applied [6, 7, 18, 19]. The brittle fracture of the filaments contributes to the degradation of the current carrying capacity of Bi2212 wire. Thus, it is important to understand the fracture strength of filaments, which is useful for predicting the irreversible current density degradation.

In order to characterize the fracture behavior of filaments, it is convenient to consider the failure probability. The Weakest Link Theory was used to model the strength of the fiber, where the survival or failure probability of chain is dependent on the element length. The Weakest Link Theory states that the survival of structure is equivalent to the survival of all elements. The relationship can be written as [20]:

$$S_{u,n}(\sigma)=\left[S_{u,r}(\sigma)\right]^n,\ n=\frac{l_n}{l_r} \tag{1}$$

where $S_{u,n}$ is the survival probability of the structure, $S_{u,r}$ is the probability of the element, l_n is the length of the chain and l_r is the length of the element (reference length). So that the exponent n is the number of elements. Using the Weakest Link Theory, Weibull provided a description of the failure

probability of structure under uniform stresses. This theory has been widely used to describe the strength of composite [21-23]. In addition, it is found that strength of composite is dependent on the number of fibers, i.e. size effect [24]. When the number of fibers exceeds a certain value, the strength of bundle will decrease [25, 26]. In order to predict of bundle strength, the hierarchical method is used by Newman and Gavbrielov [27]. However, the model neglected the influence of embedding matrix and length scaling. Pimenta and Pinho provided extended model which is more reasonable [28, 29]. Besides the size effect, the debonding and pulling out of the fiber are also considered in the model. Using the finite element method, Grail et al give a discussion about the variation of the stress concentration and the recovery length [30].

In this paper, we adopt and extended the hierarchical model proposed by Pimenta and Pinho [28] to study the strength of Bi2212 superconducting composite wire. The failure probability is derived for the filament bundle which contains three filaments. The bundle strength and size effect of the composites are obtained and compared for different case. Finally, we expand our model for the asymmetric structure and present the effect of stress concentration factor on the mean strength.

2 MODEL DESCRIPTION

There are two kind of Bi2212 composites: 7 filament bundles and 18 filament bundles. Here, we only consider the 18 bundle wire which includes 18*37 filaments and study the strength of wire by statistical analysis.

2.1 Failure analysis of bundle with three filaments

The strength of fiber bundles in composite has been studied with the hierarchical fiber bundle model [28], where the level-[i] (i>1) bundle contains two level-[i-1] bundles. Since the distribution of filaments in Bi2212 wire is specified, it is to be noted that there are three filaments in the first level. The following assumptions are adopted to analyze the strength distribution approximately.

(1). Three filaments in one level are subjected to the same stress before the failure of filaments. As filament A fails, the stress will be concentrated in the other two filaments. The discussion of failure is restricted to the control region, and the control region is given twice as long as the recovery length [28]. Based on the shear lag model, the recovery length is

$$l_{\zeta}^{(\mathrm{i})} = 2\frac{n^{(i-1)} \cdot \mathrm{A}_f \cdot \sigma}{\mathrm{C}^{(\mathrm{i}-1)} \cdot \tau_{sl}} \tag{2}$$

where the subscript ζ means recover length, A_f is the cross-sectional area of single filament, the superscripts i mean the bundle level, τ_{sl} is the shear strength, C represents the perimeter of filament bundle respectively. It is to be noted that the filament can be damaged only once in the control region due to the limitation of length.

(2). We assume that the weakest filament A will fail firstly when the stress reaches to a certain value. The location of failure is in the center of the first control length (A_1). For filaments B and C, the failure position of them are unknown. A simplification is used in the analysis: if the failure of filament occurs in a recovery length, the position of failure will be in the center of the recovery length. Then stress concentration of filament C is given in Fig. 1 as filaments A and B fail.

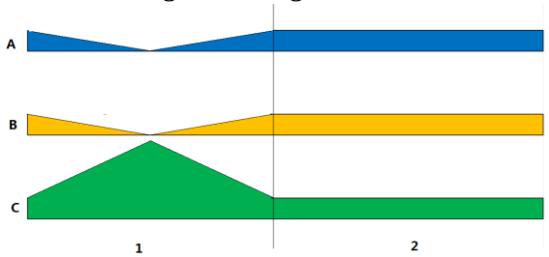

Figure 1: Stress concentration of filament C in the three filaments bundle.

As pointed out in Ref. [28], the failure of composite can be divided into stable failure and unstable failure. The unstable failure means that when the failure of the weakest filament takes place, without increasing of the longitudinal stress, the adjacent filament would break immediately due to the stress concentration. On the contrary, when the failure of weakest filament takes place, the failure of adjacent filament will occur with the increase of longitudinal stress, i.e. stable failure [28]. Since the filaments are embedded into the metal matrix, the matrix has effect on the stress concentration. We use subscripts k to represent the stress concentration as only one filament fails, and K to represent the stress concentration as two filaments fail. In the following part, $X_{u,\zeta}$ $X_{k,\zeta}$ and $X_{K,\zeta}$ stand for the strengths the segments in the recovery length under the uniform stress, the first concentration stress and the second concentration stress respectively. With a statistical analysis, the failure of filament-bundle with three filaments could be divided into following ten events (See Fig. 2). Here, we take the first situation as an example.

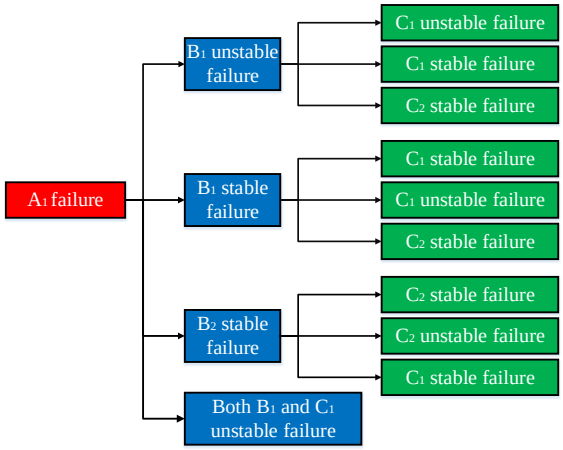

Figure 2: The events corresponding to the failure of filament bundle.

E_1: When the weakest filament segment A_1 fails, immediately, the failure of segment B_1 occurs due to the first stress concentration (unstable). C_1 also fails due to the second stress concentration (unstable).

$$\begin{aligned}\mathrm{E}_1 = \Big\{\sigma^\infty : \Big[X_{u,\zeta}^{A_1} = \sigma^\infty\Big] \wedge \Big[X_{u,\zeta}^{A_2} > \sigma^\infty\Big] \wedge \Big[X_{u,\zeta}^{B_1} > \sigma^\infty \wedge X_{k,\zeta}^{B_1} \le \sigma^\infty\Big] \\ \wedge \Big[X_{u,\zeta}^{B_2} > \sigma^\infty\Big] \wedge \Big[X_{k,\zeta}^{C_1} > \sigma^\infty \wedge X_{K,\zeta}^{C_1} \le \sigma^\infty\Big] \wedge \Big[X_{u,\zeta}^{C_2} > \sigma^\infty\Big]\Big\}\end{aligned} \tag{3}$$

where the symbol $\wedge$ means that all the cases will occur. The probability distribution function of this event F_1 can be expressed as:

$$F_1 = \Pr(\mathrm{E}_1) = \int_0^{\sigma^\infty} (dF_u)(1-F_u)(F_k - F_u)(1-F_u)(F_K - F_k)(1-F_u) \tag{4}$$

Similarly, the failure probability of the others situations can be expressed as:

$$F_2 = \Pr(\mathrm{E}_2) = \int_0^{\sigma^\infty} \left(\int_0^{\sigma} (dF_u)(1-F_u)(F_k - F_u)(1-F_u)\right)(dF_K)(1-F_u) \tag{5}$$

$$F_3 = \Pr(\mathrm{E}_3) = \int_0^{\sigma^\infty} \left(\int_0^{\sigma} (dF_u)(1-F_u)(F_k - F_u)(1-F_u)\right)(dF_u)(1-F_K) \tag{6}$$

$$F_4 = \Pr(\mathrm{E}_4) = \int_0^{\sigma^\infty} \left(\int_0^{\sigma} (F_u)(1-F_u/2)(dF_k)(1-F_u)\right)(dF_K)(1-F_u) \tag{7}$$

$$F_5 = \Pr(\mathrm{E}_5) = \int_0^{\sigma^\infty} (F_u)(1-F_u/2)(dF_k)(1-F_u)(F_K - F_k)(1-F_u) \tag{8}$$

$$F_6 = \Pr(\mathrm{E}_6) = \int_0^{\sigma^\infty} \left(\int_0^{\sigma} (F_u)(1-F_u/2)(dF_k)(1-F_u) \right) (dF_u)(1-F_K) \tag{9}$$

$$F_7 = \Pr(\mathrm{E}_7) = \int_0^{\sigma^\infty} \left(\int_0^{\sigma} (F_u)(1-F_u/2)(dF_u)(1-F_k) \right) (dF_k)(1-F_k) \tag{10}$$

$$F_8 = \Pr(\mathrm{E}_8) = \int_0^{\sigma^\infty} (F_u)(1-F_u/2)(dF_k)(1-F_u)(F_k - F_u)(1-F_k) \tag{11}$$

$$F_9 = \Pr(\mathrm{E}_9) = \int_0^{\sigma^\infty} \left(\int_0^{\sigma} (F_u)(1-F_u/2)(dF_u)(1-F_k) \right) (dF_k)(1-F_k) \tag{12}$$

$$F_{10} = \Pr(\mathrm{E}_{10}) = \int_0^{\sigma^\infty} (dF_u)(1-F_u)(F_k - F_u)(1-F_u)(F_k - F_u)(1-F_u) \tag{13}$$

It is to be noted that in the above events, the weakest segment in the bundle is A_1. For the events $\mathrm{E}_1 \sim \mathrm{E}_9$, the weakest filament may be any one of the three filaments and the second weakest filament may be the other two. As a consequence, each event only stand for the 1/12 of case. For the event E_{10}, only the weakest filament can change. Accordingly, this event stands for the 1/6 of case. The probability distribution function of bundle failure in level one can be expressed as:

$$F = 12(F_1 + F_2 + F_3 + F_4 + F_5 + F_6 + F_7 + F_8 + F_9) + 6F_{10} \tag{14}$$

The survival probability of filament under the uniform stress obeys the Weibull distribution. The distribution can be written as:

$$S_{u,n} = \exp\left[-\frac{l_\zeta}{l_r} \left(\frac{\sigma}{\sigma_0} \right)^m \right], \; F_{u,n} = 1 - \exp\left[-\frac{l_\zeta}{l_r} \left(\frac{\sigma}{\sigma_0} \right) \right]^m \tag{15}$$

where $S_{u,n}$ and $F_{u,n}$ are the survival probability and the failure probability, and σ_0, l_r and m are the Weibull parameters, respectively. σ_0 is the strength of the filament within the length of l_r. Using the Weakest Link Theory, the survival probability of stress concentration segment can be given by [28]:

$$\ln\left[S_k(\sigma^\infty) \right] = C_k \cdot \ln\left[S_u(\sigma^\infty) \right], \; C_k = \frac{k^{m+1} - 1}{(m+1)(k-1)} \tag{16}$$

2.2 The model of Bi2212 wire

Consider the Bi2212 wire with 18*37 filaments as shown in Fig. 3. In order to establish the multi-level filament bundle model, we ignore these filaments which are located in the center of the hexagon bundles. The simplified model contains 18*36 filaments. Then, level-[i] bundle may contain three or two level-[i-1] bundles.

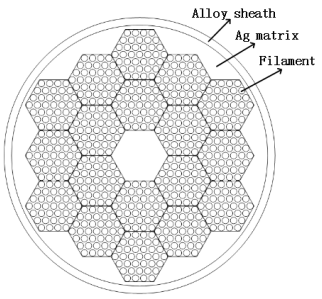

Figure 3: Cross section of Bi2212 wire.

The scheme of filament arrangement is shown in Fig. 4. In the level-[0] of the model, a Bi2212 filament is located in the center of the rhombic matrix. The level-[1] bundle is composed of the three filaments which are located at the vertices of a regular triangle. Because the filament cluster is a hexagon, as can be seen in level-[4], the three level-[3] bundles rotate around the central axis. Then, the filaments in the wire can be discretized into seven bundle levels: 3*2*2*3*3*2*3.

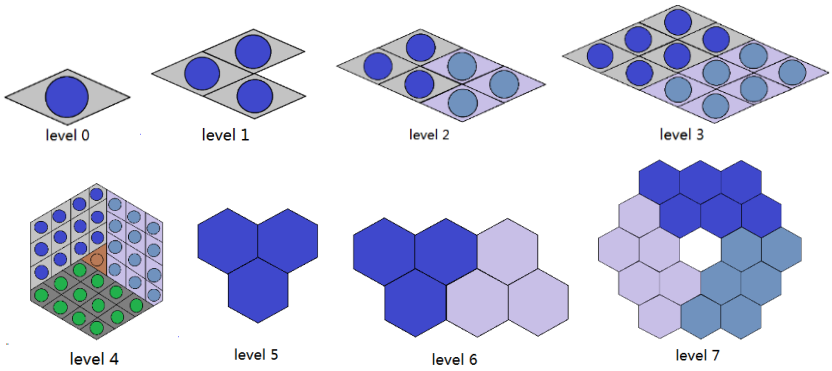

Figure 4: Scheme of bundle levels in Bi2212 wire.

2.3 Approximate analysis of hierarchical bundle

According to the crystallography, the tension strength of Bi2212 filament determined by the bond energy is about 150MPa ~ 180MPa [31]. Referring to the above data, we can find the Weibull parameters σ_0 and l_r. For the multiple integration of probability distribution, we take the absolute value of $(1-F)$ to avoid the computational error. The failure probability in control regions of level-[i] should be transformed into the reference length by the Weakest Link Theory. Then, after fitting the probability distribution function of level-[i-1] with the Weibull distribution function and updating the Weibull parameters σ_0 and m, the failure probability distribution of level-[i] can be obtained by repeating the above procedure. In order to simplify the calculation, the parameter m will not increase as it reaches a certain value. The stress concentrations factors are determined using the finite element software Abaqus [32]. The parameters used in the statistical analysis are shown in Table 1.

Mechanical properties						
σ_0	m	τ_{sl}	E_{Bi}	υ_{Bi}	E_{Ag}	υ_{Ag}
165Mpa	4.54	15Mpa	66.6Gpa	0.32	0.9Gpa	0.32
Geometry				Concentration factor		
Φ_f	V_f	l_r		k	K	
5μm	0.5	0.2mm		1.238	1.511	

Table 1: The parameters for hierarchical analysis.

3 RESULT

The numerical results of the strength distributions are shown in Fig. 5. It can be seen in Fig. 5a that with the number of filaments increasing, the probability distribution function becomes steep, which means the variability of bundle strength is reduced for the high level bundles. In addition, the tensile strengths of lower level bundles are stronger than that in single filament. When the bundles become large, the strength will decrease. One thing should be noted is that the failure probability is very close to one, and the error may be generated due to the simplification assumption of the model. The changes are quantitatively descripted in Fig. 5b, where μ is the mean strength or the expectation of the probability distribution, NUM is the number of filaments in the bundle, and CoV is the coefficient of

variation. As shown in Fig. 5b, the expectation increases in level-[1] and decreases in the other levels. The coefficient of variation decrease and approaches to a steady value with the increasing of filaments number.

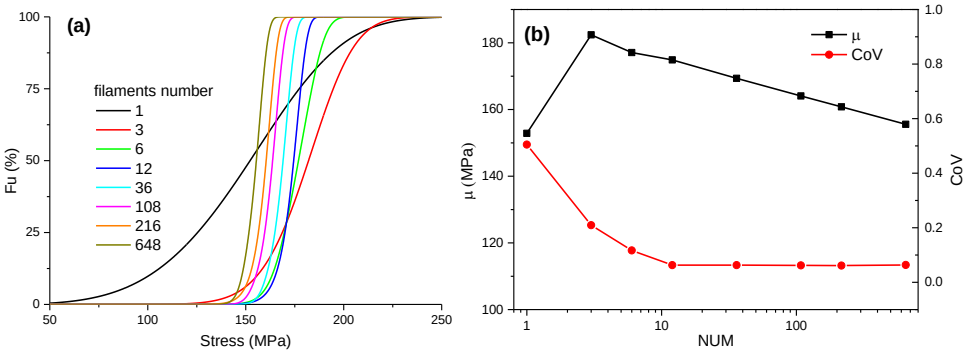

Figure 5: The numerical result of Bi2212 wire: (a) strength distributions of different levels. (b) the expectation and coefficient of variation of strength distributions.

Pimenta and Pinho discussed the strength of composites, in which the level-[i] bundle contains two level-[i-1] bundles [28]. It is interesting to compare the strength in the wire which have different filament arrangement. We make a comparison of two filament arrangement: three bundles in each level (triple) and two bundles in each level (double). The numerical results can be seen in Fig. 6. The probability distribution curve in Fig. 6a is the results of filament arrangement 2*2*2*2*2*2*2*2*2, and the curve in Fig. 6b is the results of filament arrangement 3*3*3*3*3*3. As can be seen in Fig. 6c, the strength of wire (triple) is smaller than the strength of wire (double). It is due to the reason that the number of filament in the wire (triple) increases more quickly.

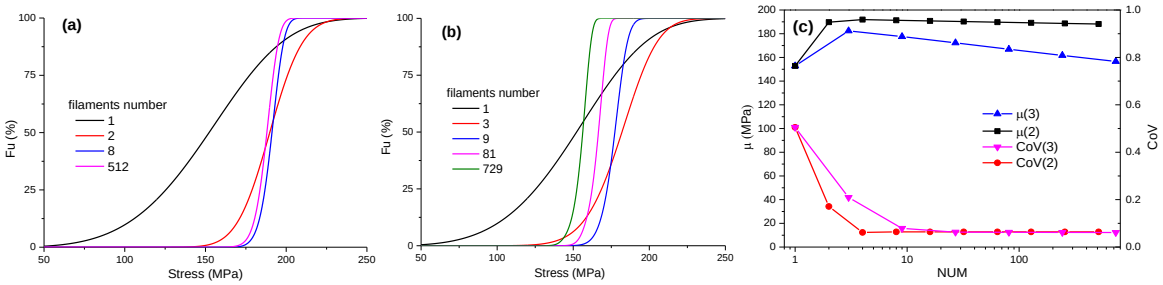

Figure 6: The comparison of results for two models: (a) the results based on the model given in Ref.[28]. (b) the present model. (c) comparison of the two models.

The results of quantitative comparison are shown in Fig. 6c. The variation tendency of the two wire is similar. The mean strength of wire (triple) is smaller and decreases more obviously with the filament number.

4 DISCUSSIONS

4.1 Effect of shear strength

The effective recovery length is determined by interface shear strength. Thus, the tension strength of bundle is dependent on the shear strength. The results for different shear strength are shown in Fig. 7. With the increasing of the shear strength, the strengths of the bundles increases. In other word, the prefect interface bonding leads to higher the tension strength. The curves of the coefficient of variation are almost the same.

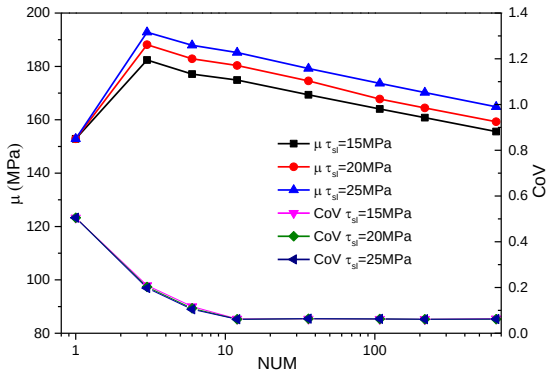

Figure 7: Expectation and coefficient of variation for different shear strength.

4.2 Non-homogeneous distribution of filament

The filaments usually have asymmetric distribution in the wire due to the fabrication and heat treatment. In the asymmetric structure, it can be found that three filaments have different relative position (See Fig. 8). Thus, the stress concentration factors are not the same for filament B and filament C. In order to analyze the effect of non-homogeneous distribution, two different stress concentration factors are studied which are given in Table 2.

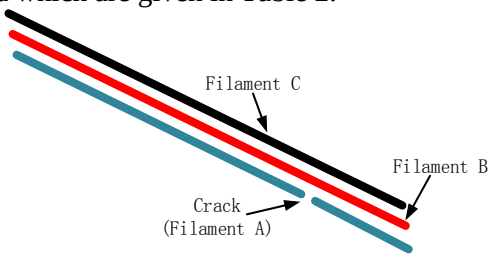

Figure 8: The schematic diagram of asymmetric structure.

When filament A fail, the stress concentration factors are different for filament B and C. Thus, it is interesting to find that the failure mode will also change for the asymmetric structure. The failure probability of filament bundle given in the above section will be modified by considering the difference between filament B and filament C.

Asymmetric distribution 1			Asymmetric distribution 2			Symmetric distribution		
k_C	k_B	K	k_C	k_B	K	k_C	k_B	K
1.2854	1.3209	2.1109	1.1971	1.2134	1.8812	1.219	1.219	1.803

Table 1: The parameters for hierarchical analysis.

For the events $E_1 \sim E_9$ the failure probability is different for filament B and filament C (the failure of the second filament), and we need to distinguish the sequence of the cases. Here, we will take the event E_1 as an example.

E_{1a}: When the weakest filament segment A_1 fails, the failure of segment B_1 occurs due to the first stress concentration (unstable). C_1 also fails due to the second stress concentration (unstable).

$$F_{1a} = \int_0^{\sigma^\infty} (dF_u)(1-F_u)(F_{k_B} - F_u)(1-F_u)(F_K - F_{k_C})(1-F_u) \tag{17}$$

E_{1b}: When the weakest filament segment A_1 fails, the failure of segment C_1 occurs due to the first concentration (unstable). Immediately, B_1 also fails due to the second stress concentration (unstable).

$$F_{1b} = \int_0^{\sigma^\infty} (dF_u)(1-F_u)\left(F_{k_C} - F_u\right)(1-F_u)\left(F_K - F_{k_B}\right)(1-F_u) \tag{18}$$

where F_{k_B} and F_{k_C} are the failure probabilities of the segments B_1 and C_1 for the first stress concentration. Then, the probability distribution function of this event could be expressed as:

$$F_1^* = F_{1a} + F_{1b} \tag{19}$$

Based on the same method, the failure probabilities of events $E_2 \sim E_9$ can be determined.

For the event E_{10}, as the failure of the weakest filament A_1 occurs, the other two filaments will also break at the same time. With a little adjustment, the probability distribution function of this event could be expressed as:

$$F_{10}^* = \int_0^{\sigma^\infty} (dF_u)(1-F_u)\left(F_{k_B} - F_u\right)(1-F_u)\left(F_{k_C} - F_u\right)(1-F_u) \tag{20}$$

The probability distribution function of asymmetric structure could be expressed as:

$$F^* = 6\left(F_1^* + F_2^* + F_3^* + F_4^* + F_5^* + F_6^* + F_7^* + F_8^* + F_9^* + F_{10}^*\right) \tag{21}$$

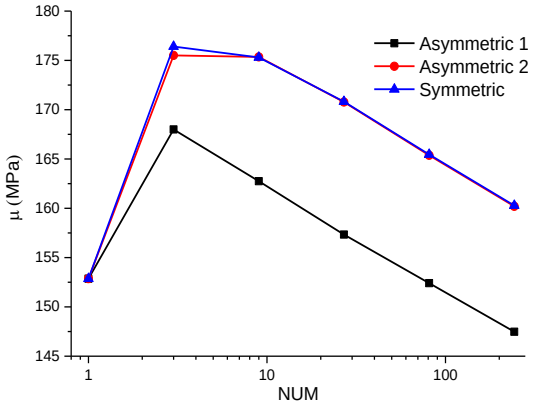

Figure 9: Strengths for the symmetric and asymmetric structures.

Consider a model which includes 243 filaments (3*3*3*3*3*3), and the level-[i] bundle contains three level-[i-1] bundles. We consider that the shear strength is invariant. The variation of mean strength of wire for different stress concentration factors can be seen in Fig. 9. The general trend is similar to that of homogeneous distribution. The mean strength increases firstly, and the decreases with the number of filaments. As expected, the strength of wire which has lower stress concentration factors has higher strength. In order to improve the strength of wire, it is important to reduce the stress concentration factor.

5 CONCLUSIONS

In this paper, we extended the statistical analysis model for the hierarchical bundles. The failure probability of filament bundle was derived for the arrangement in which one filament bundle has three filaments. The size effect of the Bi2212 wire was studied approximately with this method by considering higher level bundle includes two or three lower level bundles. The results show that the mean strength of the wire increases firstly with the filament number, and then decreases slightly. Compared to the other hierarchical structure (level-[i] bundle has two level-[i-1] bundles), the strength of wire (level-[i] bundle has three level-[i-1] bundles) is reduced. In addition, the prefect interface bonding corresponds to a higher tension strength. At last, the mean strength of asymmetric filaments was presented. It can be found that strength of wire is reduced by the higher stress concentrations factors. In order to improve the mechanical stability, it is important to reduce the stress concentration.

ACKNOWLEDGEMENTS

We acknowledge the support from the National Natural Science Foundation of China (Nos. 11472120, and 11421062), the National Key Project of Magneto-Constrained Fusion Energy Development Program (No. 2013GB110002), New Century Excellent Talents at the University of the Ministry of Education of China (NCET-13-0266) and the National Key Project of Scientific Instrument and Equipment Development (11327802).

REFERENCES

[1] H. Miao, H. Kitaguchi, H. Kumakura, K. Togano, T. Hasegawa and T. Koizumi, Bi 2 Sr 2 CaCu 2 O x/Ag multilayer tapes with J c> 500 000 A/cm 2 at 4.2 K and 10 T by using pre-annealing and intermediate rolling process, *Phys. C.*, **303**, 1998,pp. 81-90.

[2] J. Schwartz, T. Effio, X. Liu, Q. V. Le, A. L. Mbaruku, H. J. Schneider-Muntau, T. Shen, H. Song, U. P. Trociewitz, X. Wang and H. W. Weijers, High field superconducting solenoids via high temperature superconductors, *IEEE Trans. Appl. Supercond.*, **18**, 2008,pp. 70-81.

[3] H. Miao, K. R. Marken, M. Meinesz, B. Czabaj and S. Hong, Development of round multifilament Bi-2212/Ag wires for high field magnet applications, *IEEE Trans. Appl. Supercond.*, **15**, 2005,pp. 2554-2557.

[4] R. Wesche, Temperature dependence of critical currents in superconducting Bi-2212/Ag wires, *Phys. C.*, **246(1)**, 1995,pp. 186-194.

[5] T. Shen, P. Li, J. Jiang, L. Cooley, J. Tompkins, D. McRae and R. Walsh, High strength kiloampere Bi2Sr2CaCu2Oxcables for high-field magnet applications, *Supercond. Sci. Technol.*, **28**, 2015,pp. 065002.

[6] J. K. Shin, S. Ochiai, H. Okuda, Y. Mukai, H. Matsubayashi, S. S. Oh, D. W. Ha, S. C. Kim and M. Sato, Estimation of Young's modulus, residual strain and intrinsic fracture strain of Bi2212 filaments in Bi2212/Ag/Ag alloy composite wire, *Phys. C.*, **468**, 2008,pp. 1792-1795.

[7] H. W. Weijers, U. P. Trociewitz, K. Marken, M. Meinesz, H. Miao and J. Schwartz, The generation of 25.05 T using a 5.11 T Bi2Sr2CaCu2Ox superconducting insert magnet, *Supercond. Sci. Technol.*, **17**, 2004,pp. 636.

[8] N. Cheggour, X. F. Lu, T. G. Holesinger, T. C. Stauffer, J. Jiang and L. F. Goodrich, Reversible effect of strain on transport critical current in Bi2Sr2CaCu2O8 +xsuperconducting wires: a modified descriptive strain model, *Supercond. Sci. Technol.*, **25**, 2012,pp. 015001.

[9] A. Godeke, M. H. C. Hartman, M. G. T. Mentink, J. Jiang, M. Matras, E. E. Hellstrom and D. C. Larbalestier, Critical current of dense Bi-2212 round wires as a function of axial strain, *Supercond. Sci. Technol.*, **28**, 2015,pp. 032001.

[10] R. Bjoerstad, C. Scheuerlein, M. Rikel, A. Ballarino, L. Bottura, J. Jiang, M. Matras, M. Sugano, J. Hudspeth and M. Di Michiel, Strain induced irreversible critical current degradation in highly dense Bi-2212 round wire, *Supercond. Sci. Technol.*, **28**, 2015,pp. 062002.

[11] E. B. Callaway, G. Naderi, Q. Van Le and J. Schwartz, Statistical analysis of the relationship between electrical transport and filament microstructure in multifilamentary Bi2Sr2CaCu2Ox/Ag/Ag–Mg round wires, *Supercond. Sci. Technol.*, **27**, 2014,pp. 044020.

[12] C. Dai, B. Liu, J. Qin, F. Liu, Y. Wu and C. Zhou, The Axial Tensile Stress–Strain Characterization of Ag-Sheathed Bi 2212 Round Wire, *IEEE Trans. Appl. Supercond.*, **25**, 2015,pp. 1-4.

[13] X. Lu, L. Goodrich, D. van der Laan, J. Splett, N. Cheggour, T. Holesinger and F. Baca, Correlation Between Pressure Dependence of Critical Temperature and the Reversible Strain Effect on the Critical Current and Pinning Force in Wires, *IEEE Trans. Appl. Supercond.*, **22**, 2012,pp. 8400307.

[14] Z. Wang, H. Yong and Y. Zhou, Degradation of critical current in Bi2212 composite wire under compression load, *Appl. Math. Mech. -Engl. Ed.*, **(under review)**,

[15] D. Liu, J. Xia, H. Yong and Y. Zhou, Estimation of critical current distribution in Bi2Sr2CaCu2O x cables and coils using a self-consistent model, *Supercond. Sci. Technol.*, **29**, 2016,pp. 065020.

[16] D. Liu, H. Yong and Y. Zhou, Analysis of Critical Current Density in Bi2Sr2CaCu2O8+ x Round

Wire with Filament Fracture, *J. Supercond. Nov. Magn.*, **29**, 2016,pp. 2299-2309.
[17] Y. Lu, Z. Wang, H. Yong and Y. zhou, Modeling effects of gas bubbles on the mechanical behaviors of Ag/Bi-2212 round wires using a double cantilever beam bridge model, *Cryogenics.*, **77**, 2016,pp. 65-73.
[18] X. Wang, Y. X. Li and Y. W. Gao, Mechanical behaviors of multi-filament twist superconducting strand under tensile and cyclic loading, *Cryogenics.*, **73**, 2016,pp. 14-24.
[19] H. Yong, P. Yang, C. Xue and Y. Zhou, Fracture behavior of filament in Nb 3 Sn strands with crack-bridging model, *Fusion Eng. Des.*, **102**, 2016,pp. 66-73.
[20] W. Weibull, A statistical distribution of wide applicability, *J. Appl. Math.*, **103**, 1951,pp. 293-297.
[21] W. A. Curtin, Stochastic damage evolution and failure in fiber-reinforced composites, *Adv. Appl. Mech.*, **36**, 1998,pp. 163-253.
[22] S. Pradhan, A. Hansen and B. K. Chakrabarti, Failure processes in elastic fiber bundles, *Rev. Mod. Phys.*, **82**, 2010,pp. 499.
[23] S. L. Phoenix, P. Schwartz and H. H. Robinson, Statistics for the strength and lifetime in creep-rupture of model carbon/epoxy composites, *Compos. Sci. Technol.*, **32**, 1988,pp. 81-120.
[24] I. J. Beyerlein and S. L. Phoenix, Statistics for the strength and size effects of microcomposites with four carbon fibers in epoxy resin, *Compos. Sci. Technol.*, **56**, 1996,pp. 75-92.
[25] M. R. Wisnom and D. Green, Size effects in the testing of fibre-composite materials, *Compos. Sci. Technol.*, **59**, 1999,pp. 1937-1957.
[26] T. Okabe and N. Takeda, Size effect on tensile strength of unidirectional CFRP composites—experiment and simulation, *Compos. Sci. Technol.*, **62**, 2002,pp. 2053-2064.
[27] W. I. Newman and A. M. Gabrielov, Failure of hierarchical distributions of fibre bundles. I, *Int. J. Fract.*, **50**, 1991,pp. 1-14.
[28] S. Pimenta and S. T. Pinho, Hierarchical scaling law for the strength of composite fibre bundles, *J. Mech. Phys. Solids.*, **61**, 2013,pp. 1337-1356.
[29] S. Pimenta and S. T. Pinho, An analytical model for the translaminar fracture toughness of fibre composites with stochastic quasi-fractal fracture surfaces, *J. Mech. Phys. Solids.*, **66**, 2014,pp. 78-102.
[30] G. Grail, S. Pimenta, S. T. Pinho and P. Robinson, Exploring the potential of interleaving to delay catastrophic failure in unidirectional composites under tensile loading, *Compos. Sci. Technol.*, **106**, 2015,pp. 100-109.
[31] Z. Han, P. Skov-Hansen and T. Freltoft, The mechanical deformation of superconducting BiSrCaCuO/Ag composites, *Supercond. Sci. Technol.*, **10(6)**, 1997,pp. 371.
[32] L. Mishnaevsky and P. Brøndsted, Micromechanisms of damage in unidirectional fiber reinforced composites: 3D computational analysis, *Compos. Sci. Technol.*, **69**, 2009,pp. 1036-1044.